Real-Time Monitoring of Laser Transformation Surface Hardening of Ferrous Alloys

Zhiyue Xu and Claude B. Reed

Technology Development Division, Argonne National Laboratory,
9700 S. Cass Avenue, Building 360, Argonne, IL 60439

Keng H. Leong

Applied Research Laboratory, The Pennsylvania State University
State College, PA 16804

presented at International Congress on Applications of Lasers and Electro-Optics (ICALEO'99), San Diego, CA, Nov. 15-18, 1999.

Real-Time Monitoring of Laser Transformation Surface Hardening of Ferrous Alloys

Zhiyue Xu and Claude B. Reed

Technology Development Division, Argonne National Laboratory
9700 S. Cass Avenue, Building 309, Argonne, IL 60439

Keng H. Leong

Applied Research Laboratory, The Pennsylvania State University
State College, PA 16804

ABSTRACT

An infrared process monitor was used to monitor in real-time the infrared emissions during laser transformation surface hardening (LTSH) of gray cast iron and 1045 steel. The signal from the monitor was correlated with the hardness and case depth of the laser-treated tracks. Test data show that a linear relationship exists between the monitor output DC level voltage and hardness up to the maximum hardness possible and also between the monitor output DC level voltage and case depth. This simple relationship of the monitor voltage signal with hardness and case depth makes it easy to monitor process hardness, case depth and quality in real time. A calibration test on prototypic material can be used to determine at what voltage level melting occurs and the heat treating process quality can be monitored easily by setting an upper and lower bound for the voltage signal. The monitor is also capable of tracking changes in surface quality or flatness of the part that is being treated.

Key words: Laser process monitor, infrared emission, transformation surface hardening, ferrous alloys

I. INTRODUCTION

In mechanical systems, many moving components such as cam or ring gears must have a very hard surface to resist wear , along with a tough interior to resist the impact that occurs during operation. One of widely used processing techniques to realize the above combination of hard surface and tough interior is transformation surface hardening of the material, i.e. selective austenitization and martensitation of local surface region by rapid heating and cooling. The conventional methods used to harden the surface of the ferrous materials include flame and induction hardening. Case hardened depths of several millimeters are obtained but with significant thermal distortion of the components such that rework is usually required.[1,2] Laser transformation surface hardening is an alternate technique that selectively hardens the wear surface only with the rest of the component providing the heat sink. This self-quenching eliminates the need to use oil or water quenching baths. Most attractively, laser surface hardening generates low thermal distortion so refinishing of the part can be eliminated. As the use of laser surface hardening technology increases, so does the need for reliable methods for process monitoring.

For quality control of laser transformation surface hardening, the surface hardness as well as case depth are of interest. Surface hardness may be measured on-line by a hardness tester, but the measurement adds to cycle time since it is not carried out in real-time. The conventional methods of measuring case depth, such as chemical, mechanical, visual, and Eddy current method, are either destructive, cumbersome or not real-time[3]. The acoustic emission signals generated during phase transformation in metals and alloys were studied by many researchers [4-7]. The acoustic signals were detected and used to qualitatively determine the phase transformation and process defects such as cracks and porosity. Miller and Wineman [8] used manganese phosphate, a coating generally used to help couple the laser beam power into the metal surface, as the basis of a visual quality control for surface hardening of the steering gear housing. A bluish-black coloring of the treated area, surrounded by a gray border is used to indicate a satisfactory treatment. This kind of visual quality control method usually gives a very rough control of the process results. On the other hand, for laser welding--a much highly industrial accepted process, researchers have implemented various forms of weld monitoring to collect the signals and correlate them with variations in weld quality [9-13]. For example, Leong integrated an infrared emission detector into the beam delivery optics to monitor the infrared energy signal for laser welding [14]. Sanders and Leong tested in detail the infrared weld monitor technique as a welding process monitor and correlated the simple analog output with weld penetration, weld surface quality, and surface contamination with mistagging of good welds minimized [15]. In this study, the same infrared weld monitor used to monitor laser welding is used to monitor the infrared emissions from laser beam surface hardening of ferrous alloys. The signals from the monitor then are correlated with the hardness and case depth of the laser-treated tracks. A calibration test on prototypic material can be used to determine at what voltage level melting occurs. The quality of the heat treating process can be monitored easily in real-time by setting up an upper and lower bound for the voltage signal for the acceptable hardness and effective case depth.

II. EXPERIMENTAL PROCEDURES

A pulsed 2 kW Nd:YAG laser (modified Elctrox) with fiber optic beam delivery through a 1000 μm step-index fiber was used. The output optics consist of a spherical collimating lens with a combination of a 127 mm focal length cylindrical lens and a 75 mm focal length spherical lens as shown in Figure 1. An oval beam profile was achieved by the combination. The oval beam profile was chosen because of the aspect ratio and the steepness of the irradiance gradient along the minor axis (the beam was translated parallel to the major axis) for optimal heat treatment. Treated tracks were made on 1045 steel and gray cast iron (3.10-3.50 wt% carbon content) at beam travel speeds ranging from 1 to 5 cm/s provided by moving the workpiece on a X-Y table under the stationary laser head. The average power was 1200 watts (3.0 kW peak power) at the workpiece, in which the pulse width was 2 ms and the repetition rate was 200 Hz. The pulse parameters were set to simulate the effect of a continuous wave laser taking into account the thermal relaxation time of the metal. The same pulse settings were used for both alloys. The oval beam, after being defocused, had a minor axis of 4 mm and major axis of 6 mm. The area of the oval beam was 0.75 cm^2, giving a peak irradiance of the beam of 4.0 kW/cm^2. Top gas shielding was provided by a 25 lpm flow of nitrogen in a trailing jet configuration delivered by a 0.8 cm diameter tube oriented at 15^0 from the surface and 45^0 from the horizontal and 1 cm from the beam spot. The annotated photograph of the set-up of YAG laser surface hardening is shown in Figure 2. An infrared weld monitor, successfully used to monitor weld quality, was utilized to monitor the process of surface hardening. The monitor was integrated into the Nd:YAG beam delivery optics and used oversized, off-axis optics to collect the infrared emission signal associated with the process. Monitor output voltages as a function of time were collected using data acquisition hardware and software (GW Instruments, Somerville, MA) with an Apple Macintosh computer. The data collection rate used was 2500 to 5000 Hz. The monitor system noise (standard deviation) when not surface treating was 0.20 mV. The Rockwell C hardnesses along the treated tracks were measured using a portable hardness tester.Case depths of treated tracks were determined by measuring the hardness on cross-sectioned samples. The corresponding monitor voltage for each hardness or case depth measurement on a treated track was obtained from the monitor voltage-time plot.

III. RESULTS AND DISCUSSION

Figure 3 shows the raw data from the monitor where the voltage is plotted versus time obtained for a series of tests carried out with the high power pulsed Nd:YAG laser on gray cast iron. The closely spaced pulses are the dark upper part of the chart and the DC level is the top of the white light portion of the chart. The pulses are a consequence of the pulsed beam and would not be present if a cw laser is used. The signal plots from 1045 steel show similar characteristics and therefore are not shown in this paper. The bulk hardness, case depth and the corresponding monitor output DC level voltages at various beam travel speeds are tabulated in TABLE I and II for gray cast iron and 1040 steel respectively. A column indicates whether melting of the surface occurred at low travel speeds. It is obvious that the maximum bulk hardness that can be obtained with out surface melting on a cast iron workpiece is much less than the one from 1045 steel. The maximum hardness possible without surface melting for 1045 steel is about HRC 60, but only HRC 40 for gray cast iron. It is more difficult to harden gray cast iron without surface melting because a significantly longer time-at-temperature is required to diffuse carbon atoms from the graphite flakes into the matrix during laser heating [16-18]. Plots of the bulk hardness versus monitor DC voltage level for the two alloys are shown in Figs. 4 and 5. The plots of the case depth versus monitor DC voltage level for the two materials are shown in Figs. 6 and 7. The raw data for the monitor output shows that a stable voltage is produced for treated tracks that achieved substantial hardness or case depth. In fact a linear relationship exists between voltage and hardness up to the maximum hardness possible or case depth. The high R-squared values indicate the quality of the fit. Some additional increase of hardness is provided when melting occurs. This simple relationship of the monitor voltage signal with hardness and case depth makes it easy to monitor process hardness and quality.

A calibration test on prototypic material can be used to determine at what voltage level melting occurs. The heat treating process hardness and case depth can be monitored easily by setting up an upper and lower bound for the voltage signal based on the heat treatment specifications. The Figure 8 shows a sample calibration curve for laser surface hardening of 1045 steel for the laser system used in this study. The threshold melting voltage level is 450 mV. The range of data error bars for the bounds is ± 10 mV. For instance, if the required surface hardness is around HRC 50, according to the calibration curve, the monitor DC voltage output level should be within the range of 355 to 375 mV. Processing parameters, such as beam travel speed and beam pulse power settings, can then be selected according to the required DC voltage level.

Figures 9 shows the heat treated tracks produced on a gray cast iron component. The horizontal tracks are obtained before the vertical tracks in Fig. 9. Figure 10 is the raw data from the weld monitor for the wider vertical track on the middle of the photo. The additional melting and small surface change are indicated in the monitor output by the corresponding "bumps" in the data. The "low" bump at the beginning of the data for the cast iron case is caused by the depression in the component at the top part of the photo. Hence, the monitor also tracks changes in surface quality or flatness of the part that is being treated.

IV. CONCLUSIONS

The test data obtained showed that the infrared weld monitor invented at Argonne National Laboratory for process monitoring of laser welding is also capable of monitoring the process of laser surface hardening. The linear relationship of the monitor voltage signal with hardness and case depth makes it easy to monitor process hardness, case depth and quality. It is also shown by the test data that the monitor is capable of tracking changes in surface quality or flatness of the workpiece that is being treated.

ACKNOWLEDGMENTS

This work was funded by the U.S. Department of Energy, Office of Energy Research Laboratory Technology Research Program and the Office of Transportation Technologies.

REFERENCES

1. S. Lampman, “Introduction to surface hardening of steels,” ASM Handbook, Vol. 4, Heat Treating, ASM International, Materials Park, OH. 1997, pp. 259-267.
2. T. Ruglic, “Flame hardening,” ASM Handbook, Vol. 4, Heat Treating, ASM International, Materials Park, OH. 1997, pp. 268-285.
3. C.M. Klaren, J. Deere, W. Works, and J. Nelson, “Methods of Measuring Case Depth,” ASM Handbook, Vol. 4, Heat Treating, 1997, pp. 454-461.
4. R. Liptai, H. Dunegan, and C. Tatro, “Acoustic emissions generated during phase transformations in metals and alloys,” Int. J. Nondestructive Testing 1, 1969, pp. 213-221.
5. G. Speich and R Fisher, “Acoustic emission during martensite formation in steel,” ASTM STP 505, 1972, pp. 140-151.
6. E. Kannatey-Asibu and D. Pingsha, “Analysis of acoustic emission signal generation during martensitic transformation,” ASTM J. Eng. Ind. 108, 1986, pp. 328-331.
7. X. Liu and E. Kannatey-Asibu, “ Acoustic emission from single plate martensitic transformation,” J. Appl. Mech. 58, 1991, pp. 889-893.
8. J. E. Miller and J. A. Wineman, “Laser hardening at Saginaw Steering Gear,” Metal Progress, May 1977, Vol. 111, (5), pp. 38-43.
9. A. Sun, E. Kannatey-Asibu, and M. Gartner, “Sensor systems for real-time monitoring of laser weld quality,” J. Laser Appl., Vol. 11, No. 4, August 1999, pp. 135168.
10. W. Lukens and R. Morris, “Infrared temperature sensing of cooling rates for arc welding control,” Weld. J. (Miami) January, 1982, pp. 27-33

11. H. B. Chen, L. Li, D. J. Brookfield, K. Williams, and W. M. Steen, “Laser process monitoring with dual wavelength sensors,” Proc. ICALEO 91, San Jose, CA., 1991.

12. D. U. Chang, “Monitoring laser weld quality in real time,” Indust. Laser Rev. 15 November, 1994.

13. S. Charton, Y Voisim, P. Gorria, and T. Vauzelle, “ A system for on line monitoring of pulsed laser welding processes,” J. Laser. Appl., Vol 12, No. 2, April 2000, pp. 47-53.

14. K. H. Leong, “Low cost laser weld monitoring system,” Proceedings of the Automotive Laser Applications Workshop, 1997, Novi, MI., 4-5 March, 1997.

15. P.G. Sanders, K. H. Leong, J. S. Keske, and G. Korneck, “Real-time monitoring of laser beam welding using infrared weld emissions,” J. Laser Appl., Vol. 10, No., 5, October 1998.

16. V. G. Gregson, “Laser heat treatment,” Chap. 4, Materials Processing, edited by M. Bass, Holland Publishing Company, 1983.

17. O. A. Sandven, “Laser surface hardening,” ASM Handbook, Vol. 4, Heat Treating, ASM International, Materials Park, OH. 1997, pp. 286-296.

18. P. J. Oakley, “Review of laser heat treatment and surface techniques,” Research report, The Welding Institute, November, 1980.

TABLES CAPTIONS

TABLE I. Results of laser surface hardening of gray cast iron

TABLE II. Results of laser surface hardening of 1045 steel

TABLE I. Results of laser surface hardening of gray cast iron

Travel speed (cm/s)	Monitor signal (mv)	Case depth (mm)	Hardness (HRC)	Molting (Y/N) ?
1	500	0.74	51	Y
1.5	460	0.67	47	Y
2	400	0.61	40	N
2.5	360	0.5	33	N
3	310	0.41	27	N
3.5	280	0.32	25	N
4	250	0.29	<20	N
5	200	0.20	<20	N

TABLE II. Results of laser surface hardening of 1045 steel

Travel speed (cm/s)	Monitor signal (mv)	Cass depth (mm)	Hardness (HRC)	Molten (Y/N)?
1	540	1.10	62.5	Y
1.5	520	0.98	62	Y
1.8	500	0.84	61.5	Y
2	480	0.75	60	N
2.5	410	0.63	55	N
3	380	0.51	44	N
3.5	330	0.43	38	N
4	200	0.32	23	N

FIGURES CAPTIONS

Figure 1 Layout of lenses used for surface hardening with a Nd:YAG system

Figure 2 Annotated photograph of Nd:YAG laser surface hardening

Figure 3 Monitor signals of surface hardening of gray cast iron at beam travel speed of (a) 1 cm/s, (b) 1.5 cm/s, (c) 2 cm/s, (d) 2.5 cm/s, (e) 3 cm/s, (f) 3.5 cm/s, (g) 4 cm/s, and (h) 5 cm/s.

Figure 4 Plot of average bulk hardness versus the corresponding monitor DC voltage for gray cast iron.

Figure 5 Plot of average bulk hardness versus the corresponding monitor DC voltage level for 1045 steel.

Figure 6 Plot of case depth versus monitor DC voltage level for 1045 steel

Figure 7 Plot of case depth versus monitor DC voltage level for gray cast iron

Figure 8 The calibration curve for laser surface hardening of 1045 steel with a pulsed 2 kW Nd:YAG laser

Figure 9 Photograph showing the laser heat treated tracks produced on a gray cast iron component

Figure 10 Monitor signal obtained from the vertical track in Fig. 9 at beam travel speed of 2.5 cm/s

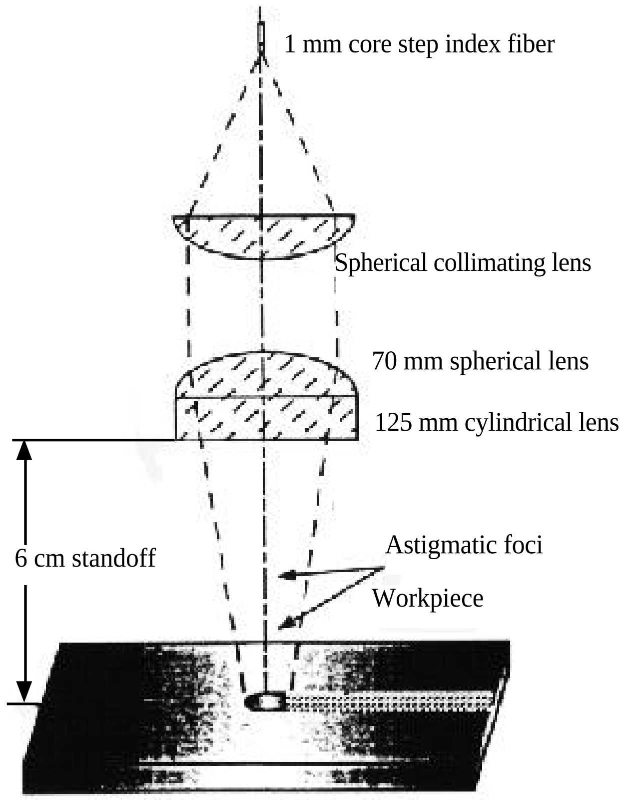

Figure 1
Zhiyue Xu
J. Laser Appl.

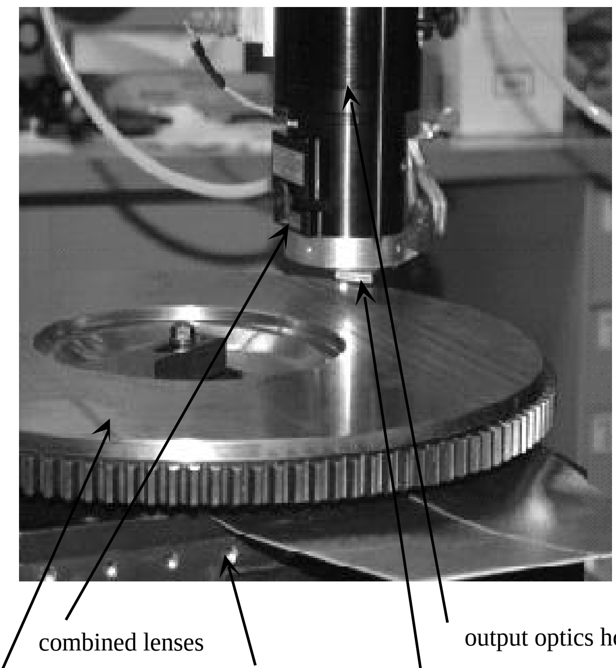

Figure 2
Zhiyue Xu

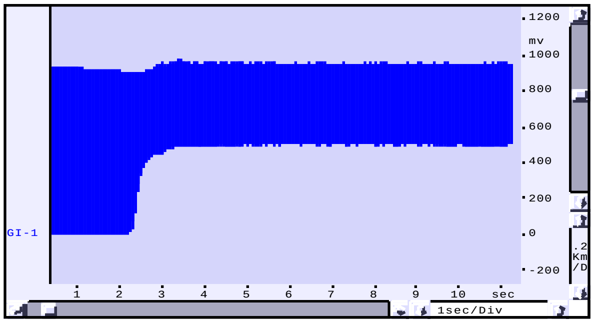

(a)

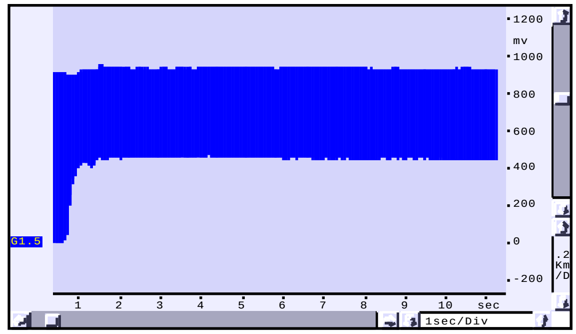

(b)

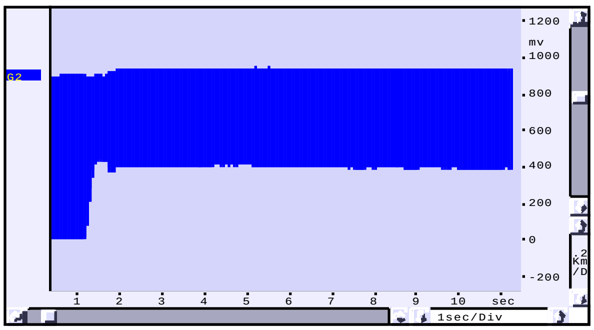

(c)

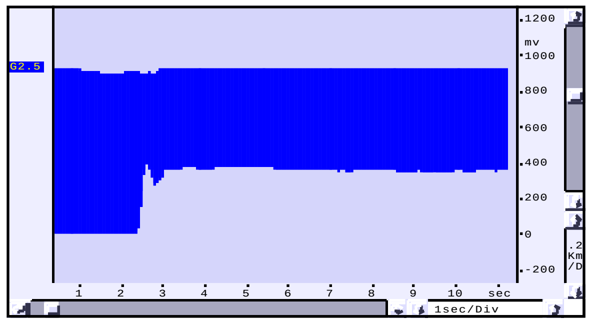

(d)

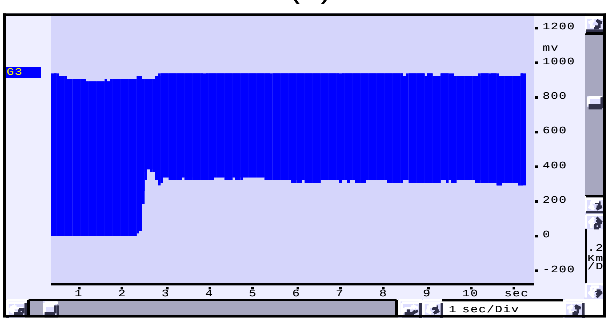

(e)

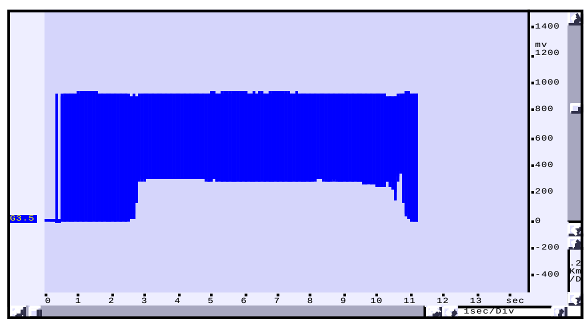

(f)

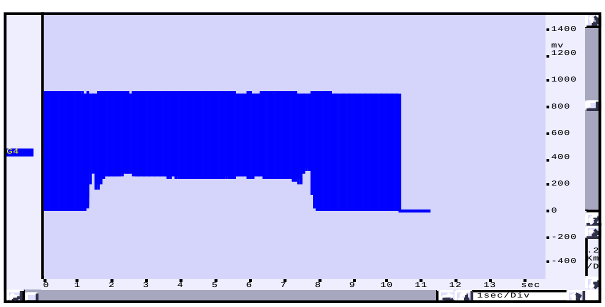

(g)

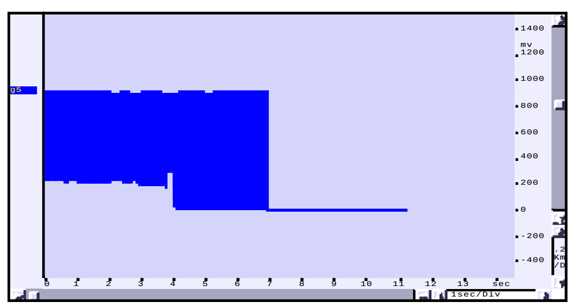

(h)

Figure 3, Zhiyue Xu

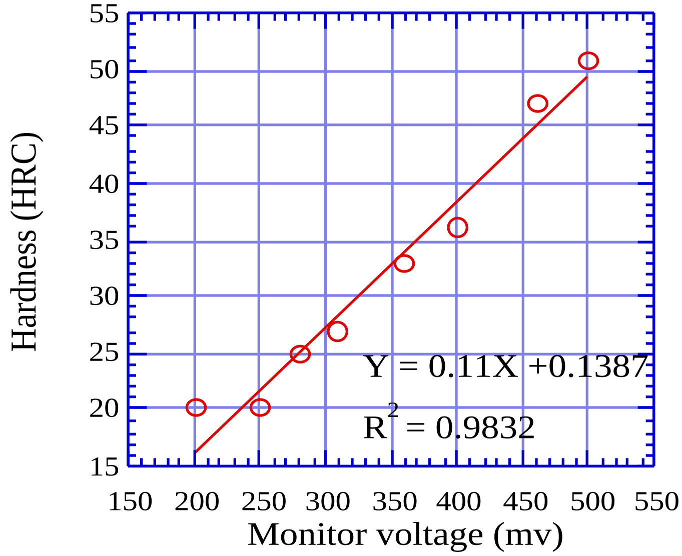

Figure 4
Zhiyue Xu

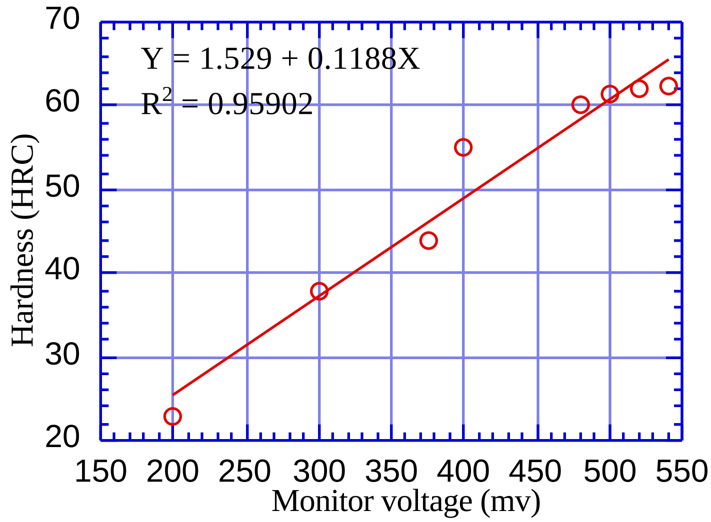

Figure 5
Zhiyue Xu

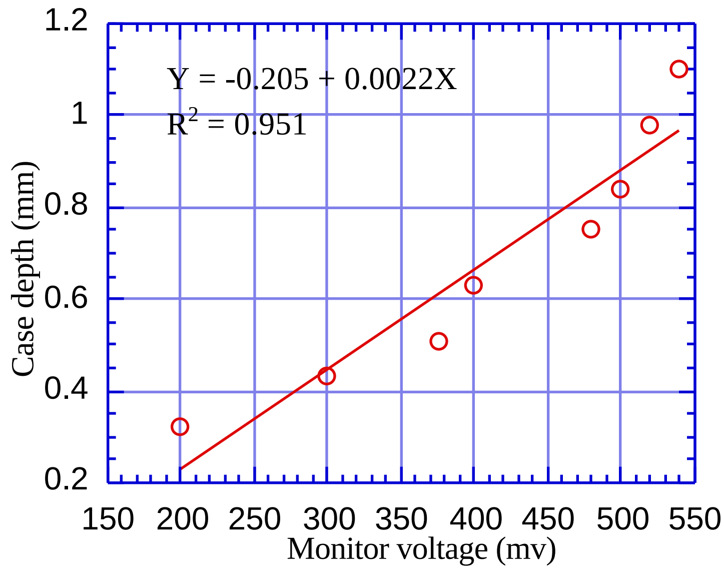

Figure 6
Zhiyue Xu

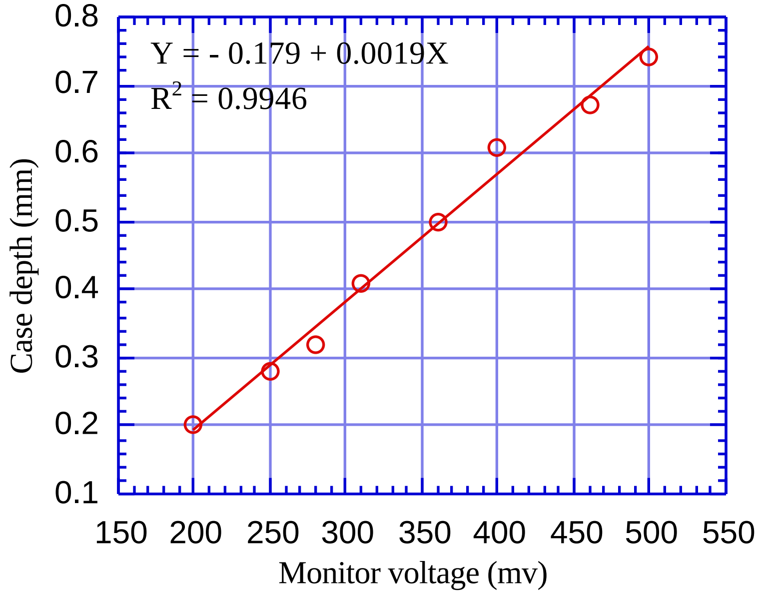

Figure 7
Zhiyue Xu

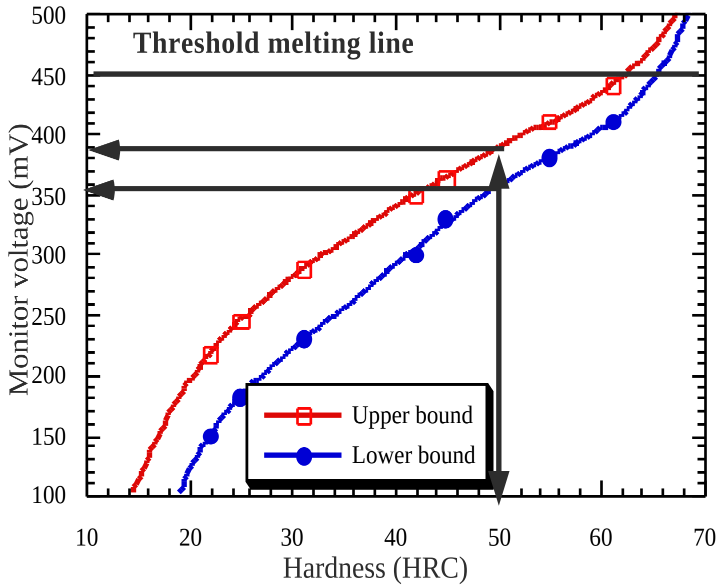

Figure 8
Zhiyue Xu

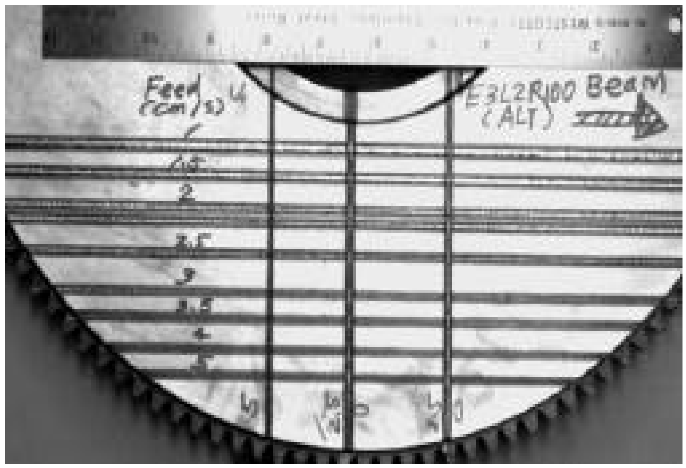

Figure 9
Zhiyue Xu

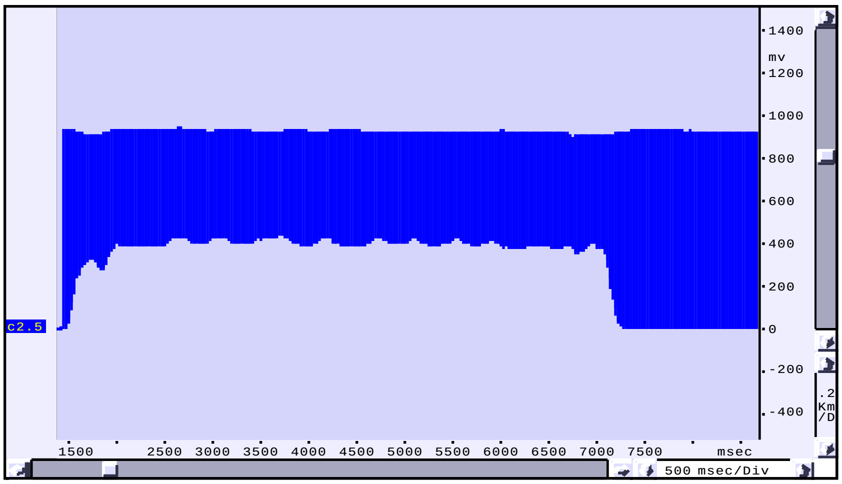

Figure 10
Zhiyue Xu